

## FLUORCAPHITE, A SECOND OCCURRENCE AND DETAILED STRUCTURAL ANALYSIS: SIMULTANEOUS ACCOMMODATION OF Ca, Sr, Na, AND LREE IN THE APATITE ATOMIC ARRANGEMENT

ANTON R. CHAKHMOURADIAN<sup>§</sup>

*Department of Geological Sciences, University of Manitoba, Winnipeg, Manitoba R3T 2N2, Canada*

JOHN M. HUGHES AND JOHN RAKOVAN

*Department of Geology, Miami University, Oxford, Ohio 45056, U.S.A.*

### ABSTRACT

Fluorcaphite is a common accessory mineral in albitite developed at the contact of quartzite and peralkaline nepheline syenites of the Lovozero complex, in northwestern Russia. The rock consists predominantly of albite, aegirine, sodic amphibole (arfvedsonite – magnesio-arfvedsonite) and narsarsukite. Fluorcaphite forms euhedral prismatic crystals up to 0.3 mm in length. Most of the crystals are homogeneous, but a few contain a resorbed core relatively depleted in Sr, Na and light rare-earth elements (LREE). This pattern of zoning arose from two overprinting episodes of metasomatism. In terms of composition, both core and rim are intermediate members of a solid solution between fluorapatite and belovite-(Ce), with the belovite content increasing toward the rim. Homogeneous crystals are compositionally equivalent to the rim, and contain approximately 50 mol.% of the belovite component. The crystal structure of the Lovozero fluorcaphite was studied by high-precision single-crystal methods and compared to that of the type material from Khibina (as re-examined in the present work). In both cases, the structure is an acentric derivative (space group  $P6_3$ ) of the  $P6_3/m$  apatite archetype. The dissymmetrization, involving loss of the center of symmetry and mirror plane, results from transformation of the Ca1 site into two non-equivalent sites tailored to accommodate different cations as substituents. The larger Ca1 site hosts a significant proportion of Sr, whereas the Ca1' site excludes Sr in the structure. The observed symmetry-breaking is subtle and poses obvious difficulties for correct space-group assignment. Potential pitfalls of space-group analysis in ordered apatite-group phases are evaluated with the Durango fluorapatite, which has a well-established  $P6_3/m$  symmetry, as an example. We found no evidence that enrichment of apatite (*sensu lato*) in Na, Sr and LREE causes phase separation and formation of intimately intergrown domains of fluorapatite and belovite.

*Keywords:* fluorcaphite, apatite, crystal structure, dissymmetrization, albitite, Lovozero, Khibina, Kola Peninsula, Russia.

### SOMMAIRE

La fluorcaphite est répandue comme minéral accessoire dans une albitite développée au contact entre fragments de quartzite et une syénite néphélinique hyperalkaline du complexe de Lovozero, dans le nord-ouest de la Russie. L'albitite contient surtout albite, aegirine, amphibole sodique (arfvedsonite – magnésio-arfvedsonite) et narsarsukite. La fluorcaphite se présente en cristaux idiomorphes prismatiques atteignant une longueur de 0.3 mm. La plupart des cristaux sont homogènes, mais quelques-uns contiennent un coeur résorbé relativement dépourvu en Sr, Na, et les terres rares légères. Ce type de zonation résulterait de la surimposition de deux événements de métasomatose. En termes de composition, le coeur et la bordure sont tous deux membres intermédiaires d'une solution solide entre fluorapatite et bélovite-(Ce), la proportion en bélovite augmentant vers la bordure. La composition des cristaux homogènes est équivalente à celle de la bordure, et contient environ 50% du pôle bélovite. Nous avons étudié la structure cristalline de la fluorcaphite de Lovozero par méthodes à précision élevée sur monocristal, et nous l'avons comparée avec le matériau provenant de la localité-type, à Khibina (que nous avons ré-examiné). Dans les deux cas, la structure est un dérivé acentrique (groupe spatial  $P6_3$ ) du groupe  $P6_3/m$  de l'apatite archetype. La dissymétrisation, impliquant une perte du centre de symétrie et du plan miroir, résulte de la transformation du site Ca1 en deux sites non-équivalents adaptés à la taille des divers cations comme substituants. Le site le plus spacieux, Ca1, contient une proportion appréciable de Sr, tandis que Ca1' exclut le Sr. La perte de symétrie est subtile, et pose un défi évident pour l'attribution du groupe spatial correct. Nous évaluons le potentiel d'erreurs dans l'analyse du groupe spatial des phases ordonnées du groupe de l'apatite avec la fluorapatite de Durango, qui possède une symétrie  $P6_3/m$  bien établie. Nous n'avons trouvé aucune indication que l'enrichissement en Na, Sr, et les terres

<sup>§</sup> E-mail address: chakhmou@ms.umanitoba.ca

rare légères dans une structure d'apatite (*sensu lato*) peut causer une séparation de phases et la formation of domaines de fluorapatite et de bélovite en intercroissance intime.

(Traduit par la Rédaction)

*Mots-clés:* fluorcaphite, apatite, structure cristalline, dissymétrisation, albitite, Lovozero, Khibina, péninsule de Kola, Russie.

## INTRODUCTION

Apatite-group minerals are sensitive indicators of changes in their crystallization milieu because of extensive atomic substitutions at the cation and anion sites. Pan & Fleet (2002) provided a detailed review of the typical substituents in the structure of natural apatites (*sensu lato*). Natural and synthetic apatites have numerous actual and potential industrial applications, *e.g.*, as phosphate, Sr and rare-earth ores, nuclear-waste repositories, phosphors, solid-state laser materials, artificial plant-growth media, and bio-implant materials. Many practically and scientifically important aspects of the crystal chemistry and physical properties of apatites have been addressed by Elliott (1994) and Kohn *et al.* (2002). Recently, there has also been a growing body of medical, anthropological and paleontological research applying "traditional" mineralogical and geochemical methods to the study of biogenic apatite (*e.g.*, Errico *et al.* 1998, Balasse *et al.* 1999, Dowker *et al.* 1999).

One aspect of the crystal chemistry of apatite-group minerals that has not been studied in adequate detail is compositionally induced structural transitions in the pseudoternary system  $\text{Ca}_5(\text{PO}_4)_3\text{X} - \text{Sr}_5(\text{PO}_4)_3\text{X} - \text{Na}_{2.5}\text{LREE}_{2.5}(\text{PO}_4)_3\text{X}$ , where LREE stands for the light rare-earth elements, and *X* is predominantly F and OH. In addition to fluorapatite and hydroxylapatite (for details on these crystal structures, see Hughes & Rakovan 2002), there are five minerals in this system: strontium-apatite, belovite-(Ce), belovite-(La), fluorcaphite and deloneite-(Ce) (Table 1). All of these minerals deviate from the archetypal structure of apatite (space group  $P6_3/m$ ) because of ordering of cations at the *A* sites (Klevtsova 1964, Pekov *et al.* 1996, Rastsvetaeva & Khomyakov 1996a, b, Rakovan & Hughes 2000). The ordering may be accompanied by changes in the coordination number of *A*-site cations, displacement of F from its ideal position at (0, 0, 1/4) along [001] and, in some cases, formation of an additional anion site at (0, 0, *z*) (*e.g.*, Rastsvetaeva & Khomyakov 1996b, Rakovan & Hughes 2000). Neither the compositions at which these ordering-induced structural transitions occur nor their dependence on crystallization parameters (especially temperature) have been ascertained.

This information is important for the practical applications of Sr–Na–REE-doped apatite-structured compounds. For example, Rakovan & Hughes (2000) suggested that it may be possible to tailor the cation order in these compounds by controlling the distribution of lanthanides between the two *A* sites by codoping

with Sr. This postulate opens intriguing avenues toward controlling the emission characteristics of apatite-type phosphors and lasers. The abundance of apatite-group phosphate minerals with Sr, Na and LREE substituting for Ca invites examination of their atomic arrangements and cation-order patterns in order to evaluate the emission parameters of similar synthetic phases.

In this study, we describe a second occurrence of the rare mineral fluorcaphite in peralkaline rocks of the Lovozero alkaline complex, in the Kola Peninsula of Russia, and provide an in-depth structural analysis of this and the type material from Khibina. We also illustrate the difficulties and ambiguities inherent in analysis of the symmetry-breaking in fluorcaphite. We combine superior refinements of the crystal structure with optimization of the ordering pattern by quadratic programming methods to more fully elucidate the atomic arrangement of this mineral.

## BACKGROUND INFORMATION

In the geological environment, the Sr(–Na–LREE)-rich apatite-group minerals are characteristic accessory constituents of peralkaline rocks, including lamproites, orangeites, foidolites and foidites, agpaite feldspathoid syenites and melasyenites, and associated pegmatites (*e.g.*, Pekov *et al.* 1995, Chakhmouradian & Mitchell 2002a, Hammond & Mitchell 2002). There are two reported occurrences of Sr-rich apatite in *bona fide* kimberlites (up to 43 wt.% SrO), and one in a granitic pegmatite (up to 20 wt.% SrO), but in all these cases, the apatite is compositionally distinct from that in peralkaline rocks (Beard *et al.* 2000, Chakhmouradian *et al.* 2002, Giller *et al.* 2002).

Fluorcaphite was initially described by Khomyakov *et al.* (1997) from peralkaline pegmatites of Mt. Koashva, in the Khibina complex in the Kola Peninsula, northwestern Russia. The simplified chemical formula of the holotype specimen is  $(\text{Ca}_{3.2}\text{Sr}_{1.2}\text{Na}_{0.3}\text{Ce}_{0.3})_{\Sigma 5}(\text{PO}_4)_3\text{F}$ ; its structure was reported as an acentric derivative ( $P6_3$ ) of the apatite archetype (Rastsvetaeva & Khomyakov 1996b). In a chemical sense, the Koashva material is an intermediate member of the fluorapatite–belovite join (and not fluorapatite–deloneite series, as suggested by Rastsvetaeva & Khomyakov 1996b), with about 63 and 33 mol.% of the respective end-members, plus a minor proportion of strontium-apatite. Note that the belovite end-member is trigonal and structurally distinct from both fluorapatite and fluorcaphite (Table 1). Prior to the discovery of fluorcaphite, Pekov *et al.*

TABLE 1. PUBLISHED STRUCTURAL DATA FOR Sr(-Na-LREE)-RICH MEMBERS OF THE APATITE MINERAL GROUP\*

Name Formula	Space group	<i>a</i> , Å	<i>c</i> , Å	Cation-site splitting (relative to archetype)	Distribution of cations over degenerate sites	Ref.
<b>Strontian fluorapatite</b> (Ca <sub>4.88</sub> Sr <sub>0.14</sub> Na <sub>0.02</sub> Ce <sub>0.01</sub> ) (P <sub>2.93</sub> Si <sub>0.02</sub> )O <sub>12</sub> F <sub>0.89</sub> (OH) <sub>0.11</sub>	<i>P6<sub>3</sub>/m</i>	9.379	6.892	none	Sr: 4% at A(1), 96% at A(2)	(1)
<b>Strontian fluorapatite</b> (Ca <sub>4.76</sub> Sr <sub>0.20</sub> Na <sub>0.04</sub> Ce <sub>0.03</sub> ) (P <sub>2.94</sub> Si <sub>0.03</sub> )O <sub>12</sub> F <sub>1.09</sub>	<i>P6<sub>3</sub>/m</i>	9.390	6.901	none	Sr: 15% at A(1), 85% at A(2)	(1)
<b>Strontian fluorapatite</b> (Ca <sub>4.46</sub> Sr <sub>0.54</sub> ) P <sub>2.92</sub> O <sub>12</sub> F <sub>0.94</sub> (OH) <sub>0.06</sub>	<i>P6<sub>3</sub>/m</i>	9.416(1)	6.924(1)	none	Sr: 13% at A(1), 87% at A(2)	(2)
<b>Strontium-apatite</b> (Sr <sub>2.88</sub> Ca <sub>1.98</sub> Na <sub>0.06</sub> LREE <sub>0.06</sub> Ba <sub>0.02</sub> ) P <sub>3.00</sub> O <sub>12</sub> F <sub>0.69</sub> (OH) <sub>0.31</sub>	<i>P6<sub>3</sub></i>	9.565(8)	7.115(3)	A(1) ⇒ A(1)' + A(1)''	Sr: 8% at A(1)', 21% at A(1)'', 71% at A(2)	(3)
<b>Fluorcapthite</b> (Ca <sub>3.16</sub> Sr <sub>1.16</sub> Na <sub>0.32</sub> LREE <sub>0.33</sub> ) P <sub>2.96</sub> Si <sub>0.06</sub> O <sub>12</sub> F <sub>0.66</sub> (OH) <sub>0.34</sub>	<i>P6<sub>3</sub></i>	9.485(3)	7.000(3)	A(1) ⇒ A(1)' + A(1)''	Sr: 45% at A(1)', 55% at A(2) Ca: 32% at A(1)'', 68% at A(2) Na: all at A(1)' LREE: all at A(2)	(4)
<b>Belovite-(Ce)</b> (Sr <sub>2.95</sub> Na <sub>0.50</sub> LREE <sub>1.00</sub> Ca <sub>0.30</sub> ) P <sub>3.00</sub> O <sub>12</sub> (OH)	<i>P3</i>	9.692(3)	7.201(1)	A(1) ⇒ A(1)' + A(1)''	Sr: 16% at A(1)'', 84% at A(2) Ca: 94% at A(1)', 6% at A(2) Na: all at A(1)' LREE: 21% at A(1)', 76% at A(1)'', 3% at A(2)	(5)
<b>Belovite-(Ce)</b> (Sr <sub>2.87</sub> Na <sub>1.06</sub> LREE <sub>1.08</sub> Ba <sub>0.11</sub> ) P <sub>3.05</sub> Si <sub>0.11</sub> O <sub>12</sub> F <sub>0.98</sub> Cl <sub>0.01</sub> (OH) <sub>0.01</sub>	<i>P3̄</i>	9.659(2)	7.182(2)	A(1) ⇒ A(1)' + A(1)''	Sr: 21% at A(1)'', 79% at A(2) Na: 94% at A(1)', 6% at A(2) LREE: 13% at A(1)', 78% at A(1)'', 9% at A(2)	(2)
<b>Belovite-(La)</b> (Sr <sub>2.86</sub> Na <sub>0.98</sub> LREE <sub>0.98</sub> Ba <sub>0.12</sub> Ca <sub>0.06</sub> Th <sub>0.01</sub> ) P <sub>2.95</sub> Si <sub>0.03</sub> O <sub>12</sub> F <sub>0.80</sub> (OH) <sub>0.18</sub>	<i>P3̄</i>	9.647(1)	7.170(1)	A(1) ⇒ A(1)' + A(1)''	not available	(6)
<b>Deloncite-(Ce)</b> (Ca <sub>1.77</sub> Sr <sub>1.18</sub> Na <sub>0.96</sub> LREE <sub>1.08</sub> K <sub>0.01</sub> ) P <sub>2.90</sub> Si <sub>0.08</sub> O <sub>12</sub> F <sub>0.72</sub> (OH) <sub>0.28</sub>	<i>P3</i>	9.51(1)	7.01(1)	A(1) ⇒ A(1)' + A(1)'' + A(1)''' + A(1)'''' A(2) ⇒ A(2)' + A(2)''	Sr: all at A(2)' Ca: 5% at A(1)', 7% at A(1)'', 20% at each A(1)''', A(1)'''' and A(2)', 28% at A(2)'' Na: 25% at A(1)', 25% at A(1)'' 50% at A(2)'' LREE: 14% at each A(1)', A(1)'''' and A(1)''', 12% at A(1)'', 47% at A(2)''	(7)

\* Only the post-1987 data are included. Z = 2 for all entries. A-cation sites in the archetypal structure (fluorapatite) are <sup>19</sup>A(1) at (1/3,2/3,-0), and <sup>17</sup>A(2) at (~0.25,-0,1/4). Degenerate cation sites in derivative structures are labeled consistently, in accord with their fractional atom coordinates, as: A(1)' (1/3,2/3,-0); A(1)'' (1/3,2/3,-1/2); A(1)''' (2/3,1/3,-0); A(1)'''' (2/3,1/3,-1/2); A(2)' (x,y,-1/4); A(2)'' (x,y,-3/4).

References: (1) Hughes *et al.* (1991), (2) Rakovan & Hughes (2000), (3) Pushcharovsky *et al.* (1987), (4) Rastsvetaeva & Khomyakov (1996a), (5) Nadezhina *et al.* (1987), (6) Pekov *et al.* (1996), (7) Rastsvetaeva & Khomyakov (1996b).

(1995) suggested, on the basis of spectroscopic data, that Sr–Na–LREE-rich apatite (~15 mol.% belowite) comprises disordered (fluorapatite-like) and ordered (belowite-like) nanodomains. If this were the case, the extent of domain development should increase with an increasing proportion of the belowite component, to the point where it would become detectable with the conventional methods of structural analysis. The atomic arrangement of the Khibina fluorcaphite was proffered by Rastsvetaeva & Khomyakov (1996b), yet few details on the symmetry-breaking and cation order in this mineral were provided.

#### OCCURRENCE

At Lovozero, fluorcaphite was found on the northern slope of Mt. Selsurt, in a porphyroblastic metasomatic rock (albitite) developed at the contact between peralkaline nepheline syenite and quartzite. The quartzite consists of a xenolith detached from metasediment-

ary country-rocks and fenitized by alkaline magma. The geology of this locality was described in detail by Pekov (2000, pp. 162–164). The fluorcaphite-bearing rock consists of large (1–3 cm) porphyroblasts of narsarsukite  $[\text{Na}_2(\text{Ti,Fe,Al,Zr})\text{Si}_4\text{O}_{10}(\text{O,F})]$  set in a massive fine-grained mesostasis of subhedral to euhedral albite (60–90 vol.%), euhedral Ti- and Zr-enriched aegirine (5–25 vol.%), and subhedral to anhedral amphibole (0–15 vol.%) (Fig. 1). The latter mineral corresponds to borderline compositions in the arfvedsonite – magnesioarfvedsonite series enriched in K and Mn (up to 2.8 and 2.5 wt.% of the respective oxides). There are two varieties of albite, differing in K and Fe contents and cathodoluminescence (CL). A K–Fe-enriched variety (dull red CL) appears to have crystallized later than the K–Fe-poor albite, showing faint bluish CL. The distribution of mafic silicates in the rock is not uniform; most of the aegirine is confined to “clots”, and is commonly replaced by the amphibole (Figs. 1a, c). Minor accessory phases include fluorcaphite, catapleiite, crypto-

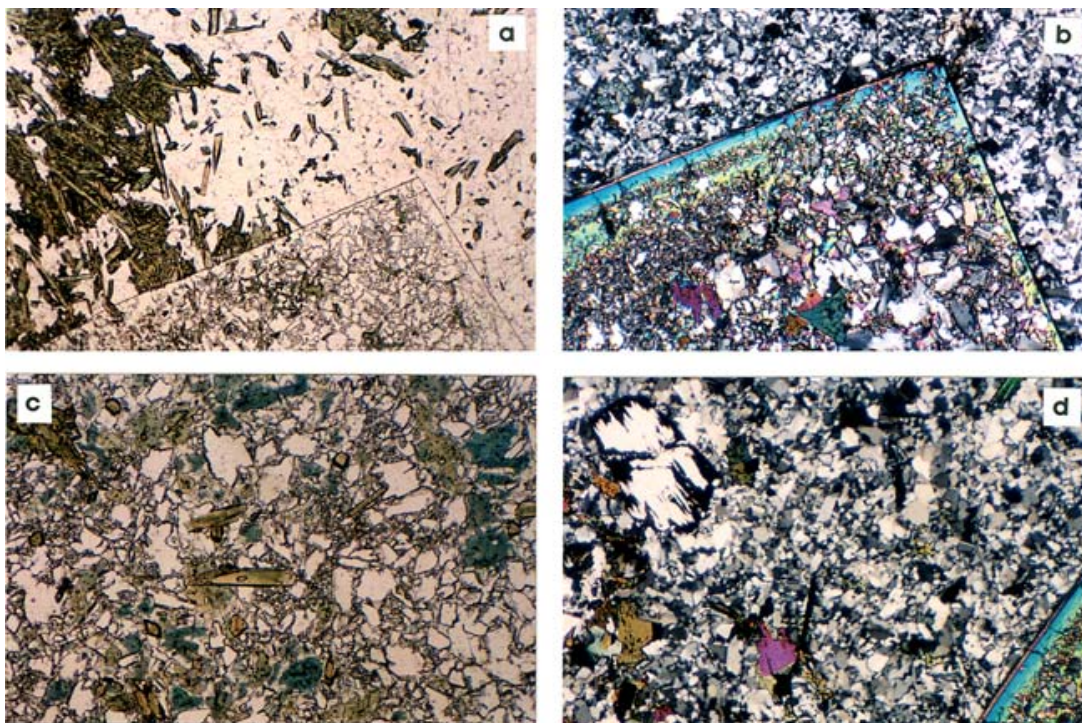


FIG. 1. Fluorcaphite-bearing albitite from Lovozero: characteristic textures. Photographs in plane-polarized light (a,c) and crossed polars (b,d). (a) “Clots” of euhedral aegirine (yellowish green) embedded in a matrix of albite (colorless); the colorless poikilitic grain at the bottom is narsarsukite. (b) Narsarsukite porphyroblast (yellow to cyan interference colors) filled with numerous inclusions of albite (white to gray) and sodic amphibole (purple and dark green). (c) Inclusions of aegirine (yellowish green), sodic amphibole (pleochroic from olive-green to grayish blue) and albite (colorless) in narsarsukite. (d) Large crystal of fluorcaphite (white, left upper corner) rimmed by rhabdophane (opaque); other minerals as in (b). Width of the field of view is 3 mm for (a,b) and 2.6 mm for (c,d).

melane, rhabdophane-(Ce) and altered (ion-leached, silicified and hydrated) pyrochlore-group minerals.

Fluorcaphite is relatively common, and forms elongate and stubby prismatic (+ hexagonal dipyramid) crystals up to 300  $\mu\text{m}$  in length; however, most crystals measure between 50 and 100  $\mu\text{m}$  in length and up to 30  $\mu\text{m}$  in width (Figs. 1d, 2a). In thin section, this mineral is colorless and can be distinguished from fluorapatite by its noticeably higher birefringence ( $\sim 0.010$ ). Some crystals of fluorcaphite enclosed in albite are surrounded by a rim of rhabdophane-(Ce) a few  $\mu\text{m}$  in width (Figs. 1d, 2b). In back-scattered-electron images (BSE), a few crystals exhibit zoning, consisting of a resorbed core and comparatively more dense euhedral rim (Fig. 2c). The contrast in average atomic number (AZ) reflects an increase in Sr and LREE (and concomitant decrease in

Ca) toward the rim. In contrast to the type material (Khomyakov *et al.* 1997), the Lovozero fluorcaphite crystallized during metasomatic reworking of the precursor quartzite. The presence of two varieties of albite, two generations of fluorcaphite, and the replacement of aegirine by sodic amphibole, indicate that the fluorcaphite-bearing rock results from an overprint of two metasomatic episodes, both involving a sodic fluid highly enriched in incompatible elements. According to the estimates of Kirnarskii *et al.* (1982), the early metasomatic paragenesis (albite + aegirine) formed at relatively high temperatures (500–600°C). Transition from this to the later-crystallized amphibole–albite paragenesis was accompanied by a significant increase in the proportion of Sr, Na and LREE in the composition of fluorcaphite. Rhabdophane-(Ce) is a product of late-

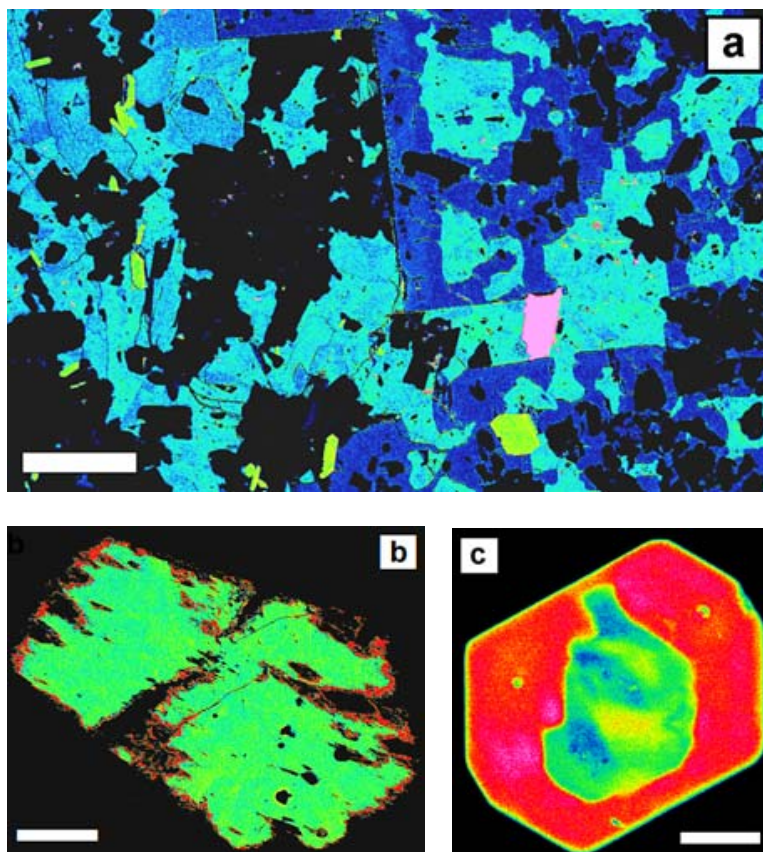


FIG. 2. Fluorcaphite from Lovozero: characteristic textures (false-color BSE images). (a) Prismatic crystals of fluorcaphite (yellowish green) embedded in a matrix of albite (black), aegirine and sodic amphibole (blue); other minerals are narsarsukite (indigo blue) and strontio-pyrochlore (mauve); scale bar 200  $\mu\text{m}$ . (b) Replacement of fluorcaphite (yellowish green) by rhabdophane (red); scale bar 100  $\mu\text{m}$ . (c) Zoning of fluorcaphite showing depletion of Sr, Na and LREE in the resorbed core (blue to green to yellow) relative to its rim (red); scale bar 10  $\mu\text{m}$ .

stage alteration of fluorcaphite that formed contemporaneously with cryptomelane and the alteration of pyrochlore (Chakhmouradian & Mitchell 2002b).

#### COMPOSITIONAL VARIATION

The chemical composition of fluorcaphite and of associated minerals was determined by wavelength-dispersion spectrometry using a Cameca SX-50 electron microprobe operated at 20 kV and 20 nA. The following standards were employed for the analysis: fluorapatite (Ca, P, F), albite (Na), barite (Ba), diopside (Si), synthetic  $\text{SrTiO}_3$  (Sr) and REE-doped glasses (La, Ce, Pr, Nd and Sm). Only those crystals were analyzed whose [001] axes are parallel or nearly parallel to the surface of the sample, in order to minimize directional diffusion of halogens under the electron beam (Stormer *et al.* 1993). The consistency of F content within compositionally equivalent zones in differently oriented crystals (estimated standard deviations for a given zone do not exceed 0.25 wt.% F) indicates that, in our case, the effect of F diffusion is negligible, if any.

Compositionally, both zoned and homogeneous crystals from Lovozero correspond to intermediate members of the fluorapatite – belovite-(Ce) series. In the zoned crystals, the proportion of belovite increases from approximately 35 mol.% in the core to 50 mol.% in the rim. The rim is indistinguishable in composition from unzoned crystals (Fig. 3). All crystals examined in the present work contain higher levels of Sr, Na and LREE (*i.e.*, a greater proportion of the belovite component) than the type material from Khibina (Khomyakov *et al.* 1997; our Table 2). The proportion of other end-members, like  $\text{Sr}_5(\text{PO}_4)_3\text{F}$  and  $\text{Ba}_5(\text{PO}_4)_3\text{F}$ , is small in fluorcaphite from both localities. Note that the Khibina fluorcaphite is chemically similar to the phosphate mineral from the Bearpaw Mountains in Montana (Fig. 3), described as Sr–Na–LREE-enriched fluorapatite (Chakhmouradian & Mitchell 1999). However, in the latter case, the small size of crystals precluded their unambiguous identification. Unfortunately, Raman microspectroscopy cannot be used to distinguish between fluorcaphite and fluorapatite because their non-polarized spectra are virtually identical. Polarized spectra in the range 50–350  $\text{cm}^{-1}$  are sensitive to the local structural environment of A-site cations and can potentially be used for that purpose (*e.g.*, Toumi *et al.* 2002).

The bulk of the Lovozero fluorcaphite is confined to a fairly narrow compositional range:  $(\text{Ca}_{2.36-2.40}\text{Sr}_{1.52-1.63}\text{Na}_{0.47-0.49}\text{Ce}_{0.26-0.29}\text{La}_{0.17-0.19}\text{Nd}_{0.07-0.08}\text{Pr}_{0.02-0.05}\text{Sm}_{0.01}\text{Ba}_{0.02-0.03})(\text{PO}_4)_3\text{F}$ . Although it was impossible to separate zoned crystals from unzoned ones, we assume that the above range represents the material extracted for single-crystal refinement of the structure. This is probably a valid assumption, considering the rarity of zoned crystals and the volumetric relationship between the relatively Sr–Na–LREE-“poor” core and Sr–Na–LREE-rich rim in such crystals.

Discrepancies between the analytical data reported for the Khibina fluorcaphite by Khomyakov *et al.* (1997) and Yakovenchuk *et al.* (1999) (particularly, in Na, La,

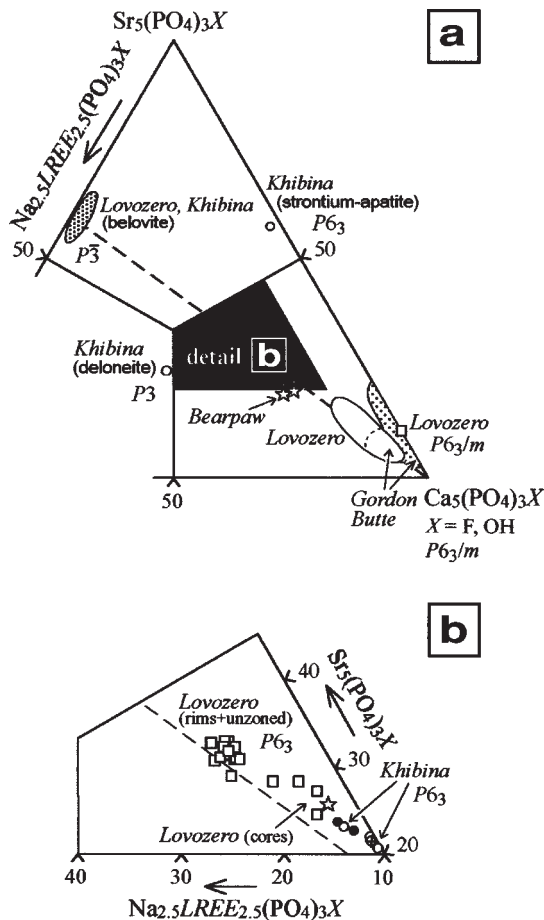


FIG. 3. Compositional variation (mol.%) and symmetry of fluorcaphite and related apatite-group minerals. Symmetry data are from the present study, Rakovan & Hughes (2000), Rastsvetaeva & Khomyakov (1996a), Pekov *et al.* (1996), and the authors' unpublished work. Compositional fields for Sr–Na–LREE-rich apatite-group minerals from Lovozero (Kola), Bearpaw Mountains and Gordon Butte (Montana) are plotted for comparison. Compositions of the Lovozero fluorcaphite are shown by empty squares, those of the Khibina fluorcaphite, by circles. Solid circles correspond to the compositions of fluorcaphite of Khomyakov *et al.* (1997) and Yakovenchuk *et al.* (1999). Open circles correspond to the average compositions of three distinct zones (with AZ increasing toward the belovite end-member), and one crossed circle, to the average composition of the Khibina fluorcaphite according to our data.

TABLE 2. REPRESENTATIVE COMPOSITIONS OF FLUORCAPHITE (1-4, 6-10) AND RHABDOPHANE-(Ce) (5)

	1	2	3	4	5	6	7	8	9	10
	L	L	L	L	L	K	K	K	K(1)	K(2)
Na <sub>2</sub> O wt.%	2.00	2.36	2.40	2.28	n.d.	1.29	1.39	1.55	1.49	1.74
CaO	28.24	21.14	21.25	20.64	0.42	32.70	30.90	28.95	30.45	30.46
MnO	n.d.	n.d.	n.d.	n.d.	0.29	n.d.	n.d.	n.d.	0.03	n.d.
SrO	21.28	26.80	25.26	24.61	4.41	17.68	18.53	19.69	19.46	20.78
BaO	n.d.	0.57	0.75	0.82	n.d.	0.07	n.d.	0.10	0.21	0.03
La <sub>2</sub> O <sub>3</sub>	2.92	4.38	4.38	4.87	18.32	3.68	4.60	5.31	3.79	2.61
Ce <sub>2</sub> O <sub>3</sub>	5.17	6.67	6.93	7.47	30.97	4.36	4.55	5.47	4.75	4.78
Pr <sub>2</sub> O <sub>3</sub>	0.49	0.75	0.59	1.24	2.39	0.21	0.21	0.32	0.48	0.34
Nd <sub>2</sub> O <sub>3</sub>	1.28	1.80	2.12	2.14	7.14	0.91	0.78	0.71	0.77	1.48
Sm <sub>2</sub> O <sub>3</sub>	n.d.	0.19	0.07	0.06	0.76	n.d.	n.d.	0.02	n.d.	0.14
SiO <sub>2</sub>	0.07	0.02	0.02	n.d.	1.41	0.51	0.64	0.82	0.55	0.57
P <sub>2</sub> O <sub>5</sub>	35.22	33.50	33.67	33.05	28.82	35.84	34.88	34.45	36.15	36.23
F	2.94	2.90	2.98	2.82	n.a.	2.50	2.36	2.32	3.54	2.17
-O=F <sub>2</sub>	1.23	1.22	1.25	1.19		1.05	0.99	0.98	1.49	0.91
Total	98.38	99.86	99.17	98.81	94.93	98.70	97.85	98.73	99.55	100.42
Na <i>apfu</i>	0.388	0.479	0.490	0.472	-	0.244	0.268	0.301	0.283	0.327
Ca	3.027	2.371	2.395	2.363	0.018	3.417	3.293	3.109	3.197	3.156
Mn	-	-	-	-	0.010	-	-	-	0.002	-
Sr	1.234	1.627	1.541	1.525	0.101	1.000	1.069	1.145	1.106	1.165
Ba	-	0.023	0.031	0.034	-	0.003	-	0.004	0.008	0.001
La	0.108	0.169	0.170	0.192	0.266	0.132	0.169	0.196	0.137	0.093
Ce	0.189	0.256	0.267	0.292	0.446	0.156	0.166	0.201	0.170	0.169
Pr	0.018	0.028	0.023	0.048	0.034	0.007	0.007	0.012	0.017	0.012
Nd	0.046	0.067	0.080	0.082	0.100	0.032	0.028	0.025	0.027	0.051
Sm	-	0.007	0.002	0.002	0.010	-	-	0.001	-	0.005
ΣA	5.010	5.029	4.999	5.010	0.985	4.991	5.000	4.994	4.947	4.979
Si	0.007	0.002	0.002	-	0.055	0.050	0.063	0.082	0.054	0.055
P	2.983	2.969	2.999	2.990	0.960	2.959	2.937	2.924	2.999	2.966
ΣT	2.990	2.971	3.001	2.990	1.015	3.009	3.000	3.006	3.053	3.021
F	0.929	0.960	0.992	0.953	-	0.771	0.742	0.735	1.097	0.664

n.d.: not detected, n.a.: not analyzed. Locality: Lovozero (L), Khibina (K). References: (1) Yakovenchuk *et al.* (1999), (2) Khomyakov *et al.* (1997). Structural formulae calculated on the basis of 8 cations (fluorcaphite) and 2 cations (rhabdophane).

Nd and F contents) prompted a re-investigation of that material. Two crystals examined in the present work exhibit a complex pattern of zoning that had not been recognized in the previous studies. The zoning does not seem to be controlled either crystallographically or morphologically. The bulk of both crystals (> 90 vol.%) comprise low- and medium-AZ material, and the proportion of the belovite component increases by *ca.* 5 mol.% from the low-AZ to high-AZ fluorcaphite (Table 2, Fig. 3). The proportion of britholite-(Ce) [LREE<sub>3</sub>Ca<sub>2</sub>(SiO<sub>4</sub>)<sub>3</sub>(OH)] also increases slightly toward the high-AZ zone. The average composition, calculated from results of a total of 15 analyses of the different zones, is: (Ca<sub>3.34</sub>Sr<sub>1.06</sub>Na<sub>0.26</sub>Ce<sub>0.16</sub>La<sub>0.15</sub>Nd<sub>0.03</sub>Pr<sub>0.01</sub>)(P<sub>2.93</sub>Si<sub>0.06</sub>O<sub>4</sub>)<sub>3</sub>F<sub>0.78</sub>(OH)<sub>0.22</sub>.

CRYSTAL-STRUCTURE REFINEMENT: EXPERIMENT

Several experiments were undertaken to evaluate the atomic arrangement of fluorcaphite. A crystal of fluorcaphite from Lovozero was mounted on a Bruker Apex CCD diffractometer equipped with MoK $\alpha$  radiation. Refined unit-cell parameters and other crystal data are listed in Table 3. Redundant data were collected for an approximate sphere of reciprocal space, and were integrated and corrected for Lorentz and polarization factors using the Bruker program SAINTPLUS (Bruker AXS Inc. 2001). The structure was easily solved by direct methods and difference-Fourier synthesis; the solution and subsequent least-squares refinement utilized programs in the Bruker SHELXTL v. 6.10 package of pro-

grams, with neutral-atom scattering factors and terms for anomalous dispersion. We took particular care in evaluating possible space-groups for fluorcaphite; a complete analysis of the symmetry-breaking from the archetypal space-group  $P6_3/m$  follows. Refinement in space group  $P6_3$  was routine in all respects. Refinement was undertaken with anisotropic thermal parameters for all non-hydrogen atoms. In Table 3, we list the pertinent data concerning the crystals chosen and results of the crystal-structure refinement; atom parameters are presented in Table 4, and selected interatomic distances, in Table 5. To further analyze the atomic arrangement of fluorcaphite, we refined the crystal structure of the neotype material from Khibina. The results of that experiment also are listed in Tables 3–5. The Tables with observed and calculated structure-factors are available from the Depository of Unpublished Data, CISTI, National Research Council, Ottawa, Ontario K1A 0S2, Canada.

It can be difficult to make the correct assignment of space group for materials that apparently exhibit subtle symmetry-breaking from a higher space-group in response to ordering of atoms, and we recognized that such is the case for fluorcaphite. The differences between the proffered  $P6_3$  atomic arrangement of fluorcaphite (Rastsvetaeva & Khomyakov 1996b) and the atomic arrangement of fluorapatite are indeed subtle and were not analyzed in that original work. For that reason, we collected data on fluorapatite from Durango, Mexico, with its well-established  $P6_3/m$  structure, using experimental parameters similar to those used for the fluorcaphite, and refined its structure in both candidate space-groups to determine the subtleties of ascribing  $P6_3$  symmetry to a mineral that actually crystallizes in space group  $P6_3/m$ . The results of those experiments

TABLE 3. EXPERIMENTAL PARAMETERS FOR FLUORCAPHITE FROM LOVOZERO (L) AND Khibina (K)

Space group: $P6_3$			
Unit-cell parameters (refined from 9,382 reflections):			
<i>L</i>	<i>a</i> 9.4456(1) Å	<i>K</i>	<i>a</i> 9.4853(2) Å
	<i>c</i> 6.9520(2) Å		<i>c</i> 6.9862(2) Å
Frame width, scan time, number of frames: 0.20°, 15 s, 4500			
Detector distance: 5 cm			
Effective transmission:			
<i>L</i>	0.748379 1.000	<i>K</i>	0.702345 1.000
$R_{int}$ (before – after SADABS absorption correction):			
<i>L</i>	0.1001–0.0166	<i>K</i>	0.0905–0.0179
Measured reflections, full sphere:			
<i>L</i>	11825	<i>K</i>	11882
Unique reflections; refined parameters:			
<i>L</i>	1045; 67	<i>K</i>	1065; 67
<i>R</i> <sub>1</sub> :			
<i>L</i>	0.0168 (1027 unique data, $I > 4\sigma_I$ ) 0.0170 (all 1045 unique data)	<i>K</i>	0.0205 (1057 unique data, $I > 4\sigma_I$ ) 0.0206 (all 1065 unique data)
Difference peaks:			
<i>L</i>	+0.49, –0.36 e <sup>–</sup> Å <sup>–3</sup>	<i>K</i>	+0.55, –0.47 e <sup>–</sup> Å <sup>–3</sup>
Goodness-of-fit:			
<i>L</i>	1.163	<i>K</i>	1.123

are given below, and illustrate the difficulties and ambiguities in space-group assignments in such cases.

## DISCUSSION OF THE ATOMIC ARRANGEMENT OF FLUORCAPHITE

### The Lovozero fluorcaphite

Details on the well-known  $P6_3/m$  atomic arrangement of fluorapatite were recently summarized by Hughes & Rakovan (2002). In this arrangement, Ca1 is at the 4*f* site at (1/3, 2/3, *z*). Symmetry-breaking to space group  $P6_3$ , as observed for fluorcaphite (Rastsvetaeva & Khomyakov 1996b), transforms the four equivalent Ca1 sites into two pairs of sites, with symmetry-equivalent sites in the two pairs related by the  $6_3$  screw axis

TABLE 4. ATOM PARAMETERS IN FLUORCAPHITE

Atom	<i>x</i>	<i>y</i>	<i>z</i>	<i>U</i> <sub>eq</sub>	Occupancy
<b>Lovozero</b>					
Ca1	2/3	1/3	0.0000(3)	0.0147(5)	Ca <sub>1,13(1)</sub>
Ca1'	2/3	1/3	0.5013(3)	0.0114(5)	Ca <sub>1,05(1)</sub>
Ca2	0.76156(3)	0.01185(3)	0.25	0.01133(10)	Ca <sub>1,328(4)</sub>
P	0.60116(5)	-0.36970(5)	0.2522(3)	0.00992(13)	P <sub>1,00</sub>
O1	0.84353(15)	0.32851(17)	0.2549(10)	0.0167(3)	O <sub>1,00</sub>
O2	0.41362(16)	-0.46562(16)	0.2537(10)	0.0197(3)	O <sub>1,00</sub>
O3	0.6532(6)	-0.2591(5)	0.0736(7)	0.0206(7)	O <sub>1,00</sub>
O3'	0.6651(6)	-0.2573(5)	0.4271(6)	0.0244(11)	O <sub>1,00</sub>
F	0	0	0.248(2)	0.0372(6)	F <sub>1,00</sub>
<b>Khibina</b>					
Ca1	2/3	1/3	-0.0017(3)	0.0148(2)	Ca <sub>1,258(8)</sub>
Ca1'	2/3	1/3	0.5013(3)	0.0124(4)	Ca <sub>1,128(8)</sub>
Ca2	0.76099(3)	0.01279(3)	0.25	0.01182(11)	Ca <sub>1,475(4)</sub>
P	0.60118(5)	-0.36967(6)	0.2522(3)	0.0102(2)	P <sub>1,00</sub>
O1	0.8441(2)	0.3286(2)	0.2561(9)	0.0176(4)	O <sub>1,00</sub>
O2	0.4143(2)	-0.4654(2)	0.2493(1)	0.0221(4)	O <sub>1,00</sub>
O3	0.6518(7)	-0.2608(6)	0.0726(6)	0.020(2)	O <sub>1,00</sub>
O3'	0.6665(7)	-0.2556(5)	0.4250(6)	0.030(1)	O <sub>1,00</sub>
F	0	0	0.246(3)	0.052(1)	F <sub>1,00</sub>

TABLE 5. SELECTED INTERATOMIC DISTANCES (Å) IN FLUORCAPHITE

Lovozero				Khibina			
Ca1–	Ca1'–	Ca1–	Ca1'–	Ca1–	Ca1'–	Ca1–	Ca1'–
O1 (×3) 2.452(5)	O1 (×3) 2.409(4)	O1 (×3) 2.481(5)	O1 (×3) 2.417(4)	O2 (×3) 2.453(5)	O2 (×3) 2.483(5)	O2 (×3) 2.479(5)	O2 (×3) 2.474(5)
O2 (×3) 2.453(5)	O2 (×3) 2.483(5)	O2 (×3) 2.479(5)	O2 (×3) 2.474(5)	O3' (×3) 2.888(5)	O3 (×3) 2.784(5)	O3' (×3) 2.909(6)	O3 (×3) 2.788(6)
O3' (×3) 2.888(5)	O3 (×3) 2.784(5)	O3' (×3) 2.909(6)	O3 (×3) 2.788(6)	Mean 2.598	Mean 2.559	Mean 2.623	Mean 2.560
Ca2–	P–	Ca2–	P–	Ca2–	P–	Ca2–	P–
F 2.3103(3)	O3' 1.526(5)	F 2.3303(4)	O3' 1.530(5)	O3' 2.360(4)	O1 1.533(1)	O3' 2.379(4)	O1 1.535(2)
O3 2.399(5)	O2 1.534(1)	O3 2.402(4)	O2 1.535(2)	O2 2.425(1)	O3 1.537(5)	O2 2.433(2)	O3 1.541(5)
O2 2.425(1)	O3 1.537(5)	O2 2.433(2)	O3 1.541(5)	O3 2.546(5)	Mean 1.533	O3 2.580(4)	Mean 1.535
O3 2.546(5)	Mean 1.533	O3 2.580(4)	Mean 1.535	O3' 2.548(4)	O1 2.689(1)	O3' 2.549(5)	O1 2.690(2)
O1 2.689(1)	O1 2.690(2)	Mean 2.468	Mean 2.480				

(Fig. 4). Thus, equivalent atoms are no longer constrained by the mirror plane or center of symmetry. The two pairs of formerly equivalent sites can accommodate different sets of substituents for the Ca atoms, adding to the robustness of the atomic arrangement of apatite (*sensu lato*).

In the holosymmetric space-group  $P6_3/m$  of fluorapatite, the single Ca1 position of rank 4 bonds to nine oxygen atoms in a tricapped trigonal prism, but with the

symmetry reduction, the single Ca1 site transforms into two distinct sites of rank 2, *i.e.*, Ca1 and Ca1'. Table 5 illustrates the results of the symmetry-breaking leading to the reduction of symmetry to  $P6_3$  in the Lovozero fluorcaphite. As noted therein, the formerly equivalent Ca1 positions degenerate to Ca1 and Ca1', with significantly different bond-distances and electron-occupancies. Most notable are the differences in bond lengths between the site occupant and the no-longer-symmetry-

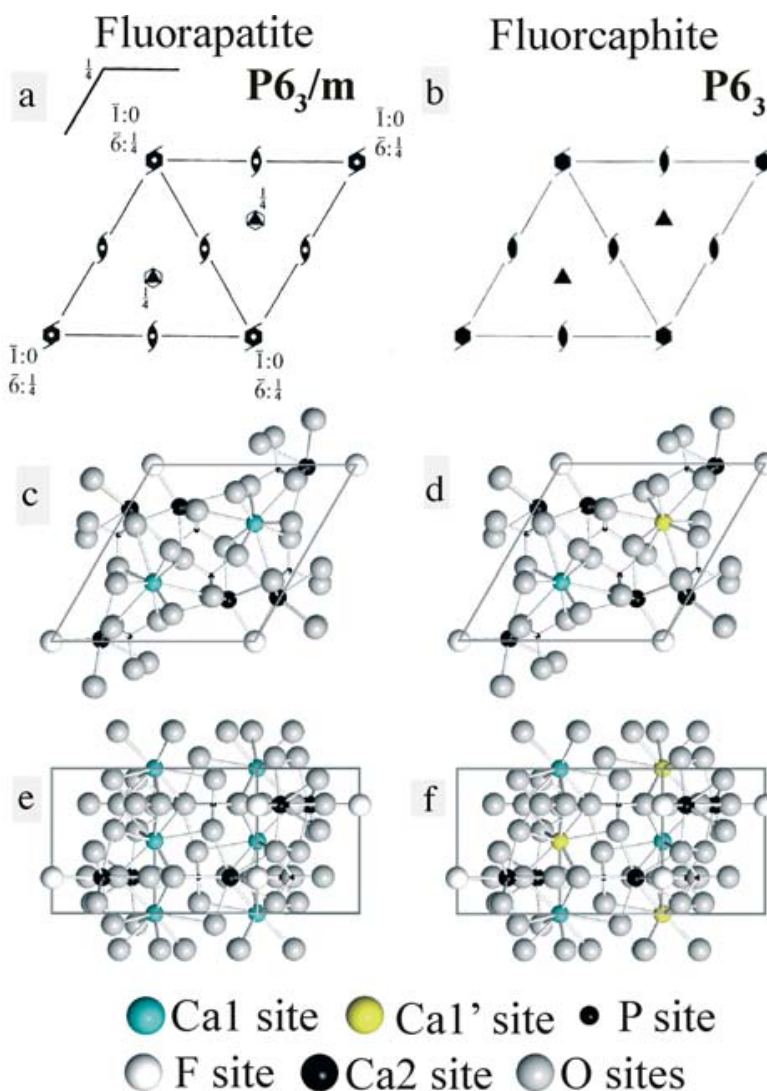


FIG. 4. Comparison of degree of order and symmetry between fluorapatite and fluorcaphite. (a, b) (001) projections of the unit-cell symmetry. (c, d) (001) projections of the atomic arrangement highlighting ordering on the Ca1 sites. (e, f) (100) projections of the atomic arrangement showing the distribution of ordered cations along the triad axes of symmetry.

equivalent O3 and O3' atoms. These bond lengths differ by  $>0.1 \text{ \AA}$  (*ca.*  $20\sigma$ ), suggesting that the symmetry-breaking results from tailoring of the two formerly equivalent sites to accommodate differing cation-substituents. That the two formerly equivalent sites contain different assemblages of cations is reinforced by the refined site-occupancies (Table 4). Using the scattering factors for Ca, the cation occupancy of the two sites refined to 1.13(1) at Ca1 and 1.05(1) at Ca1', showing the relative concentration of heavier cations at the Ca1 site. Using quadratic programming, Wright *et al.* (2000) offered a method of assigning site occupants to multiply-occupied cation sites using the results of chemical and structural data. Application of this method to the Lovozero fluorcaphite yields the optimized occupants for the Ca1, Ca1' and Ca2 sites and the following structural formula:  $(\text{Ca}_{0.96}\text{Sr}_{0.23}\text{Na}_{0.58}\text{Ce}_{0.23}\text{La}_{0.01})_{\text{Ca1}} (\text{Ca}_{1.15}\text{Na}_{0.59}\text{Ce}_{0.22}\text{Nd}_{0.04})_{\text{Ca1}'} (\text{Sr}_{2.95}\text{Ca}_{2.79}\text{La}_{0.26})_{\text{Ca2}} (\text{PO}_4)_6 \text{F}_2$ .

Sr-bearing apatite (*sensu lato*) has been extensively studied, and it is well established that Sr preferentially occupies the Ca2 site (Pan & Fleet 2002). Rakovan & Hughes (2000) showed that in strontian fluorapatite (space group  $P6_3/m$ ), Sr is virtually excluded from the Ca1 site, but in belovite-(Ce), the dissymmetrization to space group  $P\bar{3}$  allows tailoring of the individual sites to accommodate Sr and other substituents. In the Lovozero fluorcaphite, the dissymmetrization to the acentric space-group  $P6_3$  involves the loss of the center of symmetry and mirror plane. The transformation of the four Ca1 sites to two sets of two equivalent sites, and the tailoring of those sites to different substituents, allows accommodation of Sr and LREE in Ca1-equivalent sites. Sr prefers the larger Ca2 site, as it does in holosymmetric  $P6_3/m$  fluorapatite, but a significant proportion of Sr also occupies the expanded Ca1 site (0.23 *apfu*), in contrast to  $P6_3/m$  fluorapatite, in which Sr is essentially excluded from the Ca1 site. In the Lovozero fluorcaphite, however, the smaller Ca1' site excludes Sr, and is tailored to accommodate Na and the heavier lanthanide elements. Thus, the four Ca1 sites degenerate to two non-equivalent pairs with the symmetry-breaking to space group  $P6_3$ . The Ca1 site expands to include Sr, whereas the Ca1' site is smaller and devoid of detectable Sr.

#### *The Khibina fluorcaphite*

Although the structure of the Khibina material has been previously described by Rastsvetaeva & Khomyakov (1996b), a detailed analysis of the atomic arrangement was not offered. The results of the crystal-structure refinement of the neotype sample of fluorcaphite undertaken by us shows that the reasons for the symmetry-breaking in that material are similar to those discussed above for the Lovozero fluorcaphite (Tables 3–5). The Khibina fluorcaphite shows even greater differences in interatomic distances, particularly between Ca1–O3' and Ca1'–O3 (Table 5), as well as in site scat-

tering from the Ca1 and Ca1' sites (Table 4). The symmetry-breaking from space group  $P6_3/m$  is thus somewhat more pronounced in this case than in the Lovozero fluorcaphite. Assignment of cations using the quadratic programming method of Wright *et al.* (2000) gives the following structural formula:  $(\text{Ca}_{1.17}\text{Sr}_{0.42}\text{Na}_{0.39}\text{La}_{0.02})_{\text{Ca1}} (\text{Ca}_{1.76}\text{Ce}_{0.13}\text{Nd}_{0.03}\text{Pr}_{0.08})_{\text{Ca1}'} (\text{Sr}_{1.67}\text{Ca}_{3.66}\text{La}_{0.33}\text{Ce}_{0.24}\text{Nd}_{0.10})_{\text{Ca2}} (\text{PO}_4)_6 \text{F}_2$ . Like the Lovozero fluorcaphite, the Sr is ordered at the Ca1 and Ca2 sites, and excluded from the Ca1' site.

#### *Discussion of dissymmetrization from the archetypal $P6_3/m$ structure of apatite*

Our refinement of the atomic arrangement of fluorcaphite in space group  $P6_3$  demonstrates that the symmetry-breaking from  $P6_3/m$  is subtle. During crystal-structure refinements for both the Lovozero and Khibina samples, the Flack parameter refined to values within one sigma of 0.50, but significantly different from 0 or 1, suggesting that the distinction from the holosymmetric space-group may be questionable. This ambiguity was not recognized by Rastsvetaeva & Khomyakov (1996b).

Because of the difficulties in refining apatite structures in subsymmetric derivatives (*e.g.*,  $P6_3$ ) of the holosymmetric  $P6_3/m$  structure, we took particular care in refining the fluorcaphite structures, and here discuss the pitfalls and ambiguities of such refinements. To evaluate the difficulties, we refined the structure of a (nearly) spherically ground crystal of fluorapatite from Durango, with its well-established  $P6_3/m$  structure (Hughes & Rakovan 2002, and references therein), using the putative  $P6_3$  model. Such a refinement in a known-to-be-incorrect derivative of the space group  $P6_3/m$  was undertaken to illustrate the results of possible incorrect assignment of the space group to the  $P6_3$  subsymmetry. In that refinement, the Flack parameter also refined to a value within one sigma of 0.50 but significantly different from 0 or 1.

The refinement of the structure of Durango fluorapatite in space group  $P6_3$  clearly demonstrates the results of incorrect space-group assignment. In that refinement, the anisotropic thermal parameters of one of the oxygen atoms (equivalent to O3 in the  $P6_3/m$  structure) refined to non-positive-definite values, a symptom of, among other problems, incorrect space-group assignment. In common with fluorcaphite, the distances equivalent to Ca1–O in the Durango fluorapatite differ by  $14\sigma$  when its symmetry is released to  $P6_3$ , despite the well-established  $P6_3/m$  symmetry of this mineral. It is thus clear that the  $P6_3/m \Rightarrow P6_3$  symmetry reduction should be proposed and accepted with caution, as evidence of such subtle reduction in symmetry as occurs in fluorcaphite can be tenuous.

For both samples of fluorcaphite, refinements were attempted in both candidate space-groups,  $P6_3$  and  $P6_3/m$ , as noted above. Using the techniques of Hamilton

(1965), the significance of the refinement in space group  $P6_3$  over the refinement in the holosymmetric  $P6_3/m$  was confirmed at the 0.005 confidence level. However, refinement parameters such as the Flack parameter are indeed ambiguous. For Lovozero fluorcaphite, when racemic twinning was arbitrarily introduced into the refinement, the proportion of the two twin components was within  $1\sigma$  of 1:1, suggesting that the structure is actually centrosymmetric. For Khibina fluorcaphite, however, the structure was shown to consist of only one twin component, more strongly supporting the  $P6_3$  conclusion. On the basis of previous work and the results of the Hamilton (1965) significance test we thus proffer the  $P6_3$  refinements, but caution that the conclusion of acentricity is at or near the limits of detection by conventional X-ray methods.

#### SUMMARY

Our data indicate that fluorcaphite is not confined in occurrence to late-stage hydrothermal parageneses in peralkaline pegmatites. At Lovozero, this mineral formed as a product of relatively high-temperature sodic metasomatism, and contemporaneously with the bulk of the assemblage of metasomatic minerals. In terms of composition, the known examples of fluorcaphite belong to intermediate members of the fluorapatite–belovite-(Ce) series with ~35–50 mol.% of the latter end-member. The atomic arrangement of fluorcaphite is an acentric subsymmetry ( $P6_3$ ) of the  $P6_3/m$  apatite archetype. The symmetry-breaking occurs as the apatite structure adapts to the multiple substituents for Ca (primarily, Na, Sr and LREE), which require differing structural settings. Fluorcaphite accommodates these substituents by transformation of the four  $P6_3/m$ -equivalent Ca1 sites to two pairs of sites (Ca1 and Ca1'). Each of these non-equivalent sites adapts to different occupants, which is reflected in their ligation and site-scattering values. There is no evidence that Na–Sr–LREE enrichment in apatite (*sensu lato*) causes phase separation and subsequent formation of fluorapatite and belovite domains. Finally, because of the inherent difficulties in detecting minor symmetry-breaking, we suggest that the dissymmetrization to space group  $P6_3$  from the holosymmetric space-group  $P6_3/m$  cannot be considered definitive.

#### ACKNOWLEDGEMENTS

This study was supported in part by the University of Manitoba and the Natural Sciences and Engineering Research Council of Canada (ARC). The structure portion of this work was supported by NSF grant EAR-0003201 (JMH and JR). The manuscript benefitted from many constructive comments made by Ramiza Rastsvetaeva, Associate Editor Franklin F. Foit, and an anonymous referee. Editor Robert F. Martin is most

gratefully acknowledged for his continuing outstanding efforts to the science of mineralogy. Viktor Yakovenchuk is thanked for providing a neotype sample of fluorcaphite from Khibina, and Ron Chapman for his highly skilled help with the analytical work.

#### REFERENCES

- BALASSE, M., BOCHERENS, H. & MARIOTTI, A. (1999): Intra-bone variability of collagen and apatite isotopic composition used as evidence of a change of diet. *J. Archaeol. Sci.* **26**, 593-598.
- BEARD, A.D., DOWNES, H., HEGNER, E. & SABLUKOV, S.M. (2000): Geochemistry and mineralogy of kimberlites from the Arkhangelsk Region, NW Russia: evidence for transitional kimberlite magma types. *Lithos* **51**, 47-73.
- BRUKER AXS INC. (2001): SaintPlus. Bruker AXS Inc., Madison, Wisconsin.
- CHAKHMOURADIAN, A.R. & MITCHELL, R.H. (1999): Primary, apatitic and deuteric stages in the evolution of accessory Sr, REE, Ba and Nb-mineralization in nepheline-syenite pegmatites at Pegmatite Peak, Bearpaw Mts., Montana. *Mineral. Petrol.* **67**, 85-110.
- \_\_\_\_\_ & \_\_\_\_\_ (2002a): The mineralogy of Ba- and Zr-rich alkaline pegmatites from Gordon Butte, Crazy Mountains (Montana, USA): comparisons between potassic and sodic apatitic pegmatites. *Contrib. Mineral. Petrol.* **143**, 93-114.
- \_\_\_\_\_ & \_\_\_\_\_ (2002b): New data on pyrochlore- and perovskite-group minerals from the Lovozero alkaline complex, Russia. *Eur. J. Mineral.* **14**, 821-836.
- \_\_\_\_\_, REGUIR, E.P. & MITCHELL R.H. (2002): Strontium-apatite: new occurrences and the extent of Sr-for-Ca substitution in apatite-group minerals. *Can. Mineral.* **40**, 121-136.
- DOWKER, S.E.P., ANDERSON, P., ELLIOTT, J.C. & GAO, X.J. (1999): Crystal chemistry and dissolution of calcium phosphate in dental enamel. *Mineral. Mag.* **63**, 791-800.
- ELLIOTT, J.C. (1994): *Structure and Chemistry of the Apatites and Other Calcium Orthophosphates*. Elsevier, Amsterdam, The Netherlands.
- ERRICO, F., WILLIAMS, C.T. & STRINGER, C. (1998): AMS dating and microscopic analysis of the Sherborne bone. *J. Archaeol. Sci.* **25**, 777-787.
- GILLER, B., SIMMONS, W.B., FALSTER, A.U., SPRAGUE, R. & WIELKIEWICZ, T. (2002): Fluorapatite from the Emmons pegmatite, Oxford county, Maine. *J. Pegmatology* **I**(1) (available on-line at <http://www.pegmatology.com/bgillerdoc1.htm>).
- HAMILTON, W.C. (1965): Significance tests on the crystallographic  $R$  factor. *Acta Crystallogr.* **18**, 502-510.

- HAMMOND, A.L. & MITCHELL, R.H. (2002): Accessory mineralogy of orangeite from Swartruggens, South Africa. *Mineral. Petrol.* **76**, 1-19.
- HUGHES, J.M., CAMERON, M. & CROWLEY, K. (1991): Ordering of divalent cations in the apatite structure: crystal structure refinements of natural Mn- and Sr-bearing apatite. *Am. Mineral.* **76**, 1857-1862.
- \_\_\_\_\_ & RAKOVAN, J. (2002): The crystal structure of apatite,  $\text{Ca}_5(\text{PO}_4)_3(\text{F},\text{OH},\text{Cl})$ . In *Phosphates: Geochemical, Geobiological, and Materials Importance* (M. Kohn, J. Rakovan & J.M. Hughes, eds.). *Rev. Mineral. Geochem.* **48**, 1-12.
- KHOMYAKOV, A.P., KULIKOVA, I.M. & RASTSVETAeva, R.K. (1997): Fluorapatite  $\text{Ca}(\text{Sr},\text{Na},\text{Ca})(\text{Ca},\text{Sr},\text{Ce})_3(\text{PO}_4)_3\text{F}$  – a new mineral with an apatite-like structural motif. *Zap. Vser. Mineral. Obshchest.* **126**(3), 87-97 (in Russ.).
- KIRNARSKII, YU.M., KONDAKOV, YU.S. & SAVITSKII, A.V. (1982): Aegirine–albite metasomatic rocks of the Lovozero massif and its surrounding country rocks. *Dokl. Akad. Nauk SSSR* **267**, 1183-1186 (in Russ.).
- KLEVTSOVA, R.F. (1964): The crystal structure of strontium-apatite. *Zh. Strukt. Khim.* **5**, 318-320 (in Russ.).
- KOHN, M.J., RAKOVAN, J. & HUGHES, J.M., eds. (2002): Phosphates – Geochemical, Geobiological, and Materials Importance. *Rev. Mineral. Geochem.* **48**.
- NADEZHINA, T.N., PUSHCHAROVSKY, D.YU. & KHOMYAKOV, A.P. (1987): Refinement of the crystal structure of belovite. *Mineral. Zh.* **9**(2), 45-48 (in Russ.).
- PAN, YUANMING & FLEET, M. (2002): Compositions of apatite-group minerals: substitution mechanisms and controlling factors. In *Phosphates: Geochemical, Geobiological, and Materials Importance* (M.J. Kohn, J. Rakovan & J.M. Hughes, eds.). *Rev. Mineral. Geochem.* **48**, 13-49.
- PEKOV, I.V. (2000): *Lovozero Massif: History, Pegmatites, Minerals*. Ocean Pictures, Moscow, Russia.
- \_\_\_\_\_, CHUKANOV, N.V., ELETSKAYA, O.V., KHOMYAKOV, A.P. & MEN'SHIKOV, YU.P. (1995): Belovite-(Ce): new data, refined formula and the relationship to other minerals of apatite group. *Zap. Vser. Mineral. Obshchest.* **124**(2), 98-110 (in Russ.).
- \_\_\_\_\_, KULIKOVA, I.M., KABALOV, YU.K., ELETSKAYA, O.V., CHUKANOV, N.V., MEN'SHIKOV, YU.P. & KHOMYAKOV, A.P. (1996): Belovite-(La)  $\text{Sr}_3\text{Na}(\text{La},\text{Ce})[\text{PO}_4]_3(\text{F},\text{OH})$  – a new rare-earth mineral of the apatite group. *Zap. Vser. Mineral. Obshchest.* **125**(3), 101-109 (in Russ.).
- PUSHCHAROVSKY, D.YU., NADEZHINA, T.N. & KHOMYAKOV, A.P. (1987): Crystal structure of strontium-apatite from Khibina. *Kristallogr.* **32**, 891-895 (in Russ.).
- RAKOVAN, J. & HUGHES, J.M. (2000): Strontium in the apatite structure: strontian fluorapatite and belovite-(Ce). *Can. Mineral.* **38**, 839-845.
- RASTSVETAeva, R.K. & KHOMYAKOV, A.P. (1996a): Crystal structure of deloneite-(Ce), a highly ordered Ca-analogue of belovite. *Dokl. Ross. Akad. Nauk* **349**, 354-357 (in Russ.).
- \_\_\_\_\_ & \_\_\_\_\_ (1996b): Structural features of a new naturally occurring representative of the fluorapatite–deloneite series. *Crystallogr. Rep.* **41**, 789-792.
- STORMER, J.C., PIERSON, M.L. & TACKER, R.C. (1993): Variation of F and Cl X-ray intensity due to anisotropic diffusion in apatite during electron microprobe analysis. *Am. Mineral.* **78**, 641-648.
- TOUMI, M., SMIRI-DOGGUY, L. & BULOUE, A. (2002): Structure cristalline et spectres Raman polarisés de  $\text{Na}_{1.5}\text{Sm}_{8.5}(\text{SiO}_4)_6\text{FO}$ . *Ann. Chim. Sci. Mat.* **27**(2), 17-26.
- WRIGHT, S.E., FOLEY, J.A. & HUGHES, J.M. (2000): Optimization of site-occupancies in minerals using quadratic programming. *Am. Mineral.* **85**, 524-531.
- YAKOVENCHUK, V.N., IVANYUK, G.YU., PAKHOMOVSKIY, YA.A. & MEN'SHIKOV, YU.P. (1999): *Minerals of the Khibiny Massif*. Zemlya Press, Moscow, Russia (in Russ.).

Received November 7, 2003, revised manuscript accepted January 17, 2005.